Stress Relaxation in Entangled Comb Polymer Melts

T. A. Yurasova,† T. C. B. McLeish,*,‡ and A. N. Semenov§

Department of Physics, University of Sheffield, Sheffield S3 7RH, U.K., IRC in Polymer Science and Technology, University of Leeds, Leeds LS2 9JT, U.K., and Physics Faculty, Moscow State University, 117234 Moscow, Russia

Received May 16, 1994; Revised Manuscript Received August 26, 1994®

ABSTRACT: The rheological behavior of a branched polymer melt is studied theoretically, based on the extension of the primitive path and tube model. We have developed the method to evaluate the stress relaxation moduli and the viscosity of a comb polymer melt and to find out how the result is affected by various improvements in the theory. A carefully calculated form of the path length effective potential is used, including the logarithmic term (which can be derived from a detailed description of the relaxation of a branch) and also allowing for tube dilation (i.e., we take into account that constraint release speeds up reptation). Two qualitatively different types of long-time behavior are predicted, depending on whether the comb backbones are self-entangled or not. Both have already been observed in previously published data.

1. Introduction

Rheological properties of concentrated polymer systems are essentially determined by the effect of entanglements. The mobility of each macromolecule in a melt is restricted topologically by numerous knots and entanglements with the neighboring chains. In consequence the response of the melt to an external strain is observed to be highly sensitive to the chain length and to the molecular topology. It is now established that these topological interactions give rise to the steep dependence of viscosity η on molecular weight M ($\eta \approx M^{3.4}$). For branched polymers, on the other hand, experiments give approximately exponential dependences of the melt viscosity η and the stress relaxation time τ on the length of the branches.[1]

Theoretical study of these dependences[2-5] is based on the extension of the primitive path or tube model which was introduced first in the context of linear polymers.[6-9] Each macromolecule is regarded as if it moves along an imaginary tube formed by all the surrounding entanglements. A long-scale motion of a macromolecule can be thought of as reptation or creeping along the so-called primitive path,[6,8] which is the shortest line connecting two chain ends and topologically equivalent to the chain itself.[10] An important parameter of the model is N_e, the average number of monomers in a chain segment between two neighboring entanglements. (Then the tube diameter is $a \sim N_e^{1/2} l$, where l is the Kuhn length.) Alternatively, one can look at a macromolecule as if placed in a network of entanglements;[9] in other words, one can assume that all the entanglements form a sort of periodic space lattice in which the macromolecule moves.

These concepts have been extended and applied to star-shaped polymers by a number of authors.[2-5,11,12] A natural way of tackling the problem has been to assume that relaxation of a star in a melt is fully determined by progressive renewal of orientation of the branches by escaping from their original tubes, just as for linear polymers. The distinction is that the reptation mechanism of linear polymers is suppressed by the long-chain branching of the molecule. The remaining dynamical process which allows stress relaxation is the fluctuation of primitive path length by retraction of the chain length along its tube, followed by a subsequent exploration of a new tube. This is illustrated schematically in Figure 1 for the equivalent case of an entangled side branch of a comb (see below). Just as the reptation process can be mapped onto the 1-dimensional diffusion of a Brownian particle,[7] so the retraction mechanism becomes the diffusion of the chain end in a mean field effective potential $U(m)$. m refers here to the dimensionless length of primitive path[6] L explored by the chain end during a retraction. It may be made dimensionless in terms of the tube diameter, a, via $m = L/a$. $U(m)$ reflects the influence of the surrounding chains on the branch relaxation, providing the necessary statistical weight against rare retractions of the free end.

Thus the problem has been reduced to the choice of the potential field. The dependence of $U(m)$ on the path length m proves to be nearly quadratic.[2,3] This reflects the rubber-elastic origin of the potential in curvilinear extensions of the chain along its primitive path. $U(m)$ can be derived from the Boltzmann equation:

$$P(m,n) \sim \exp[-U(m)/T] \quad (1)$$

where $P(m,n)$ is the path length probability distribution for the given length n of the branch. Helfand and Pearson[4,5,11] and then Rubinstein and Helfand[12] derived an equation for $P(m,n)$, and solved it to find the potential. As a result, they obtained approximately exponential dependences of the viscosity η and the stress relaxation time τ on the length of the branch (with some power factors weakly depending on n). However, they did not take into account the boundary conditions for the probability, and although they came to realistic estimations for η and τ, the theory allows further improvement. In fact, theoretical results for η and τ appear to be quite sensitive to the choice of the potential field. In refs 13 and 14 one of us has considered the problem in detail and has derived more carefully the effective potential $U(m)$. Some later studies[15] support our results. The relevant calculations are discussed briefly in Appendix 1.

On the other hand, it has been suggested[16-18] that, for a realistic account of experiments on branched polymers, the effect of "constraint-release" or "tube dilation" should be also taken into account: the stress contribution from a given chain can be relaxed by the dynamics of its environment as well as by its own diffusion. The point is that constraint release may actually facilitate retraction because relaxed parts of the chains act as a solvent for the remainder. When this is important, the model of entangled

† University of Sheffield.
‡ University of Leeds.
§ Moscow State University.
® Abstract published in *Advance ACS Abstracts*, October 15, 1994.

0024-9297/94/2227-7205$04.50/0

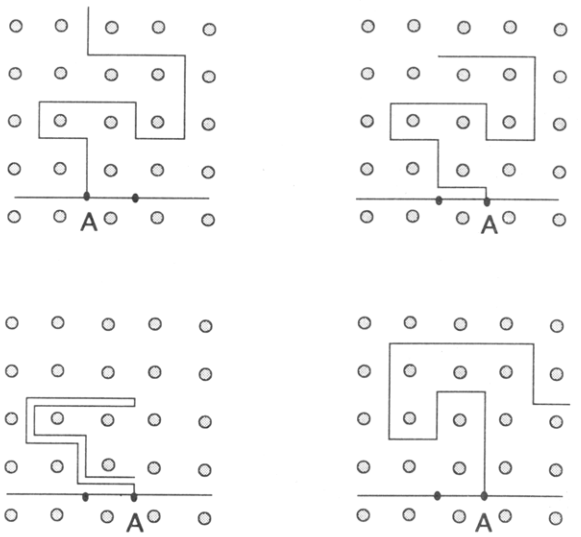

Figure 1. A polymer chain with a branch in a network of entanglements. Relaxation of the branch to the new equilibrium state is shown.

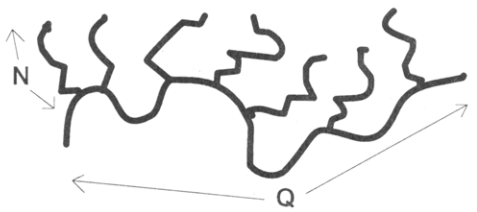

Figure 2. Notation used to describe the structure and topology of model comb polymers. N is the degree of polymerization of the arms, and Q that of the backbone. The number of side branches in the molecule is $(Q/q) - 1$.

dynamics in a fixed network will not account for the cooperative relaxation which obtains in the melt. However, this shortcoming can be disguised in practice by allowing freedom in the choice of prefactor to the potential $U(m)$. This idea has been applied to linear polymers by Marrucci[16] and then to H-polymers[17] and to star polymers[18] by McLeish and Ball, who found that it strongly modifies the Kramers[19] process by which stress relaxes. In the case of well-entangled branched polymers, the effect of constraint release may change the predicted relaxation times and viscosities by many orders of magnitude.

The current theory for entangled dynamics of star arms is as a consequence now well-tested by experiment and can be applied to more complex molecular topologies. An obvious candidate is the comb architecture. Some excellent experimental studies on the rheology of well-characterized comb polymers exist in the literature.[20,21] Moreover, this level of complexity motivates an extension of the theoretical model to deal with the motion of the molecular "backbones" at long times or low frequencies. In this paper we shall look at the rheology of a comb polymer allowing for increase in the tube diameter during relaxation of the branches.

2. Method

We summarize our model's notation schematically in Figure 2 in terms of the comb structures. N is the degree of polymerization of the side branches, assumed monodisperse, from which we define the dimensionless arm length $n = N/N_e$. At any time, such a side branch may occupy a primitive path length s, which is a fluctuating quantity. We likewise normalize s by the size of the effective network a such that $m = s/a$. The constant a can be thought of as a tube diameter, corresponding to the lattice spacing of Figure 1. The degree of polymerization of the backbone is denoted by Q and the number of monomers on the backbone between side branches by q. We consider the case of well-entangled side arms and backbone, $N \gg N_e$ and $Q \gg N_e$.

Let us assume that an external force has been applied to a comb polymer melt for some period, causing a shear strain. The resulting stress relaxation process can be understood by looking at how different parts of a comb macromolecule in the melt gradually relax after the external force has ceased. Figure 1 illustrates the relaxation. Stress carried by side branches is relaxed by reconfigurations involving more or less of the arm just as for entangled star polymers. Stress contributions from parts near the free end are relaxed typically much faster than those from nearer the branch point. Occasionally a path length fluctuation will permit the entire side branch to explore a new configuration, spreading over from one channel of the network into another and allowing the branch point itself to move one lattice spacing (tube diameter). Hence, relaxation of the backbone is controlled by repeated transfers of the branches into further channels of the lattice. The longest relaxation time τ of a comb, equivalent to the backbone relaxation time τ_{bb}, must, therefore, be limited up from below by the relaxation time of a branch, τ_{br}.

There is a straightforward scaling estimation for τ,[13] assuming that the backbone itself *reptates* (conditions for the validity of this assumption will be examined below). At time scales longer than the relaxation time of an arm, the slow variables of the system are the positions of the branching points along the backbone. The only topological interactions effective at these time scales will be the entanglements between backbones because all other polymer segments renew their configurations on much faster time scales. Let q be the number of monomers in a main chain segment between two neighboring branching points, whereas Q is the number of monomers in the main chain as a whole. Then, summing up the friction at all the branching points, one will come to

$$\tau \sim (Q/N_e)^2(Q/q)\tau_{br} \tag{2}$$

At these time scales, the polymer behaves like a reptating chain with all the effective friction concentrated in Q/q "beads" at the branch points. Meanwhile τ_{br} can be calculated via Kramers' method for a particle diffusion through a potential barrier[19] (see Appendix 2).

This yields the basic information for understanding the melt rheology. The stress relaxation modulus $G(t)$ can be expressed[1,5] in terms of the unrelaxed fraction of the chain, $f(t)$, at the moment t:

$$G(t) = G_0 f(t) \tag{3}$$

where

$$G_0 = \lim_{\omega \to \infty} G(\omega)$$

Then the zero-shear-rate viscosity is

$$\eta(0) = \int_0^\infty G(t)\, dt \tag{4}$$

and the complex modulus is

$$G(\omega) = i\omega \int_0^\infty G(t) \exp(-i\omega t)\, dt \tag{5}$$

Thus, for the branches, the unrelaxed fraction $f(t)$ is[5,13]

$$f_{br}(t) = \int_0^1 F_{br}(x,t)\,dx \qquad (6)$$

$$x = 1 - m/n\zeta$$

where $F_{br}(x,t) = \exp[-t/\tau_{br}(x)]$ is the probability that the branch end will never reach the point x till the moment t, given that initially (at $t = 0$) the end was at the point $x = 0$, and $n\zeta$ is the dimensionless equilibrium path length for the side branches (Appendix 1). From Kramers' barrier-tunneling result

$$\tau_{br}(x) = (1/D)\int_0^x \exp[U(x')/T]\,dx' \int_{-\infty}^{+\infty} \exp[-U(x')/T]\,dx' \qquad (7)$$

Here D is the diffusion coefficient of the branch retraction motion; $D \sim N^{-1}$ (see Appendix 2).

Meanwhile, Doi–Edwards theory for linear polymer melts can be applied to the backbones:[6]

$$f_{bb}(t) = \Phi_{DE}(t) \equiv \sum_{p\ \mathrm{odd}} [8/(\pi^2 p^2)] \exp(-p^2 t/\tau) \qquad (8)$$

where τ should be the backbone relaxation time given by eq 2.

Taking into account that G_0 in eq 3 is actually different for branches and backbones, namely, $G_{0br} \cong G_{00}N/(N + q)$, and $G_{0bb} \cong G_{00}q/(N + q)$, where $G_{00} = (G_{0br} + G_{0bb}) \sim T/(N_e^{2\beta})$ (ref 24), we can investigate, for various frequency ranges, which of the two relaxational processes is more important for the melt rheology.

3. Results

3.1. A Comb in a Matrix. In this section we discuss briefly and compare with experiments our previous results[13,14] for a comb in a matrix; i.e., we consider the comb polymer melt, neglecting the effect of the tube dilation. As mentioned above, this is not inapplicable to experimental data if the coefficient of the molecular weight in $U(m)$ is kept free, in which case the logarithmic corrections to the potential will be detected in the dependence of τ on M. For this case we use the potential $U(m)$ with quadratic and logarithmic terms (see Appendix 1).

The complex melt viscosity, $\eta(\omega) = \eta_{br}(\omega) + \eta_{bb}(\omega)$, is shown qualitatively in Figure 3. Apparently, the backbones' relaxation gives the major contribution to $\eta(\omega)$ at low frequencies of a periodic external stress; relaxation of the branches, in contrast, becomes more important at higher ω.

The predictions of the theory agree with some experimental results. For instance, the longest stress relaxation time (in the logarithmic scale) is

$$\log \tau = \mathrm{const} + (N/N_e)(\zeta^2/2) + \log(N/N_e) \qquad (9)$$

for $N_e \ll N$; $Q,q = \mathrm{const}$. This is plotted in Figure 4a for $z = 6$ ($\zeta^2/2 \approx 0.22$) and compared to the data of Roovers and Toporowski.[20] The slope of the straight line for $Q,N = \mathrm{const}$

$$\log \tau = \mathrm{const} - \log(q/N_e) \qquad (10)$$

agrees with experiments as well (see Figure 4b). However, we had to readjust the model parameters in the theoretical formulas in such a way that experimental and theoretical values for $\log(\tau)$ were the same at one of the points. In the next section we discuss how allowing for the tube dilation may help to improve the theory and explain the full relaxation spectrum.

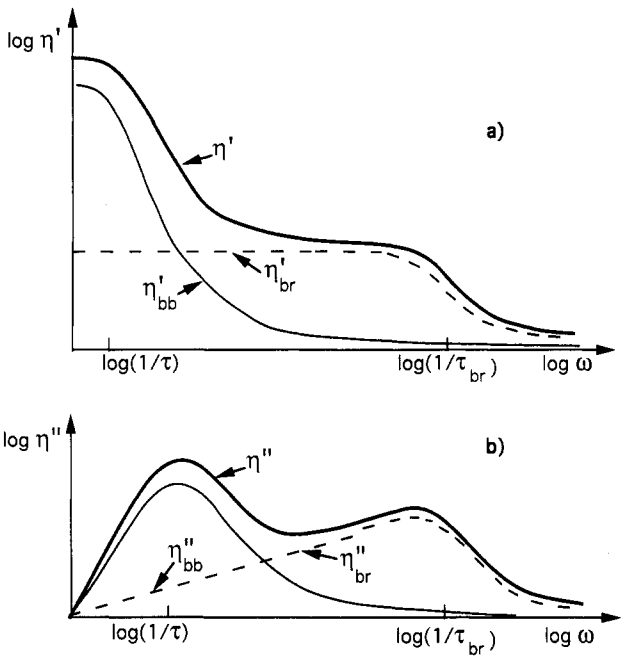

Figure 3. Frequency dependence of the real (η') and imaginary (η'') parts of the comb polymer melt viscosity. Contributions to the viscosity due to the backbones' relaxation (η_{bb}, thin solid line) and due to the branches' relaxation (η_{br}, dashed line) are shown.

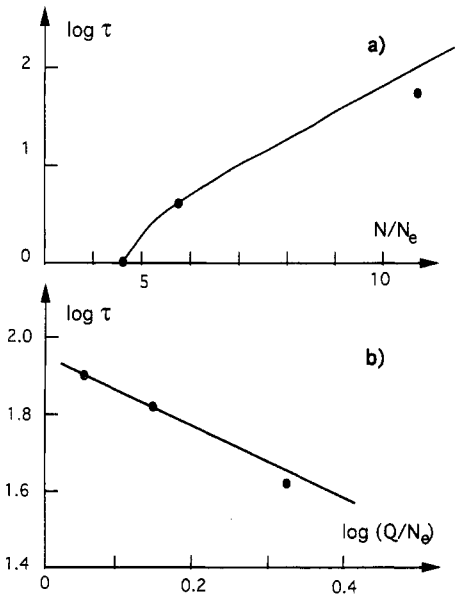

Figure 4. Longest stress relaxation time, τ, in a comb polymer melt versus the number of entanglements N/N_e per branch (a); the same versus the number of entanglements q/N_e per backbone segment between two neighboring branching points (b). Our theory[13,14] (solid lines) is compared with experiments[20] (circles). The model parameters are chosen to provide the fitting at the point $N/N_e = 3.56$ (a) and $\log(q/N_e) = 0.16$ (b).

3.2. A Comb in a Melt (Tube Dilation). Now we suggest that the tube diameter a (or, in other words, the parameter N_e) effectively increases during the branch relaxation.[16,17] The reason is that, at every moment, an unrelaxed part of the branch appears to be effectively diluted in a solvent of already relaxed parts of the chains; this must speed up its further relaxation. We exploit the fact that, under dilution with solvent, the plateau modulus $G_0 \sim c^\alpha$ with $\alpha \approx 2$ and the wide separation of relaxation time scales in a branched melt[7,18,24] in two ways. First, for

times up to τ_{br}, the stress is proportional to the *square* of the unrelaxed fraction of the molecule $f(t)$, so that $G(t) \sim [f(t)]^2$. Second, the dilution effect is taken as a widening of the tube at longer time scales, so modifying the effective potential $U(m)$. The effective value of N_e increases throughout the relaxation, so that the total primitive path length n becomes dependent on the current extent of relaxation, $m(t)$. This program was worked through for the case of a melt of stars by Ball and McLeish in ref 18; the present case differs in the m dependence of the unrelaxed fraction.

The unrelaxed fraction of a comb is given by

$$f(t) = \frac{Q + (Q/q)M(t)/\zeta}{Q + (Q/q)N} = \frac{q + M(t)/\zeta}{q + N} \qquad (11)$$

$$M(t) = m(t)N_e$$

and determines the effective concentration of entanglements, $c_{eff} \approx N_{e0}/N_e(t)$. Thus, from the self-consistent equation, $f(t) = c_{eff}(t)$, we find the path length dependence of the entanglement parameter $N_e(m)$ and, therefore, of the relative branch length $n(m)$:

$$n(m) = Am[(1 + Bm)^{1/2} - 1]^{-1} \qquad (12)$$

with

$$A = 2N/(q\zeta)$$

and

$$B = 4N_{e0}(1 + N/q)/(q\zeta)$$

Hence, the effective increment $dU(m)$ in the potential (see Appendix 1) will be

$$dU/T = [(1/A)(1 + Bm)^{1/2} - 1/A - z - (m + 1/z)^{-1}]\, dm \qquad (13)$$

which leads to the following form of the potential:

$$U(m)/T = \frac{2}{3AB}(1 + Bm)^{3/2} - (\zeta + 1/A)m - \ln(m + 1/\zeta) + \text{const} \qquad (14)$$

instead of eq A.2.2).

Now, based on a similar procedure to that already described (see eqs 3–8), the rheology of the melt can be investigated. We should note though that there may be two possibilities depending on the values of c_{eff} at τ_{br}, the effective concentration of entanglements per backbone. This is explained in the next section.

3.3. Backbone-Dynamics: Long-Time Modes. The considerations of constraint release during the retraction-dominated arm relaxations considered above lead to two different cases for the long-time relaxation:

Case 1. The backbones are mutually entangled; i.e., $Qc_{eff} \gg N_e$ (and, therefore, $N_{e0}(N/q + 1) \ll Q$). In this case the backbones will be involved in a kind of reptation motion, although in a wider tube, so a rescaled Doi–Edwards theory will apply (cf. eq 8):

$$G(t) \approx [f(t)]^2\Phi_{DE}(t) \qquad (15)$$

$$\Phi_{DE}(t) = \frac{8}{\pi^2}\sum_{p\ \text{odd}}\left[\frac{1}{p^2}\right] e^{-p^2t/\tau}$$

with relaxation time τ given by a modified form of eq 2,

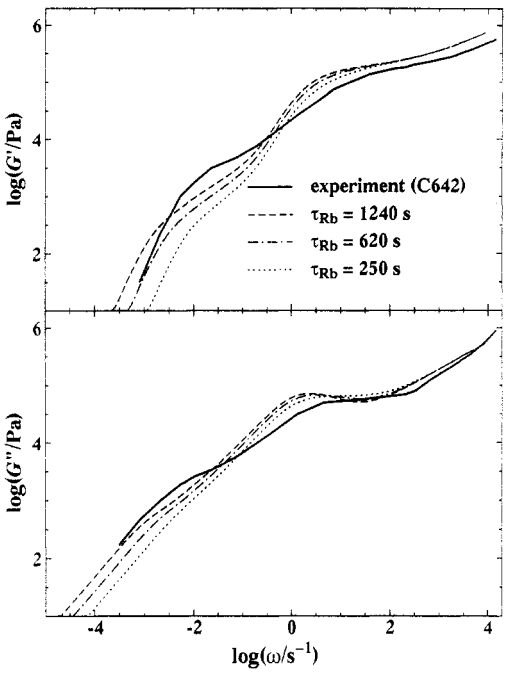

Figure 5. Frequency dependence of the storage G' (a) and loss G'' (b) moduli for the comb denoted C642 by Graessley and Roovers. The figure shows a comparison of our theory to experiments[21] for the case of mutually diluted backbones ($Q/N_e = 14$, $Q_{eff} = 3$). A number of choices of prefactor for the effective diffusion of a branch point are made and compared.

in which N_e is replaced by the effective value of N_e evaluated at τ_{br}:

$$N_e(\tau_{br}) = N_{e0}\left(\frac{q}{q + N}\right) \qquad (16)$$

Case 2. The backbones are mutually unentangled; i.e., $N_{e0}(N/q + 1) \gg Q$. Then they will relax freely in a kind of high-friction medium, with friction effectively located at the branching points only. Therefore, a Rouse model can be used:

$$G(t) \approx [f(t)]^2\sum_p \exp(-2tp^2/\tau_{Rb}) \qquad (17)$$

where τ_{Rb} is a Rouse time for the backbone; it can be expressed in terms of the friction coefficient at a branching point, μ_{br}, and the number of branches, (Q/q):

$$\tau_{Rb} \cong \frac{\mu_{br}a_{br}^2}{3\pi^2T}(Q/q - 1)^2 \qquad (18)$$

Estimating $\mu_{br} \cong 3T/D_{bb} \cong (3T/a^2)\tau_{br}$, where $D_{bb}\tau_{br} \cong ql^2$. This represents one natural choice for the effective step a branch point makes between retractions, though we note that dilution would enlarge the tube at long times, thus speeding up the long-time Rouse motion of the backbone. It is chosen in this case because the branch points are closer together than the tube diameter for the experimental polymer to which we compare this case below. The correct physical choice in the other limit of $ql^2 \gg a^2$ would be $D_{bb}\tau_{br} \cong a^2$. In practice, there is some uncertainty in how these two limits plus the effect of tube dilation combine to produce an effective diffusion constant for the branch points. In particular, if the backbones are not self-entangled, then the later stages of the arm retractions must also be, leading to an early "disentanglement transition" which mildly renormalizes the effective friction constant of the branch point. The choices of long Rouse time in Figure 5 reflect variations in the $O(1)$ coefficient

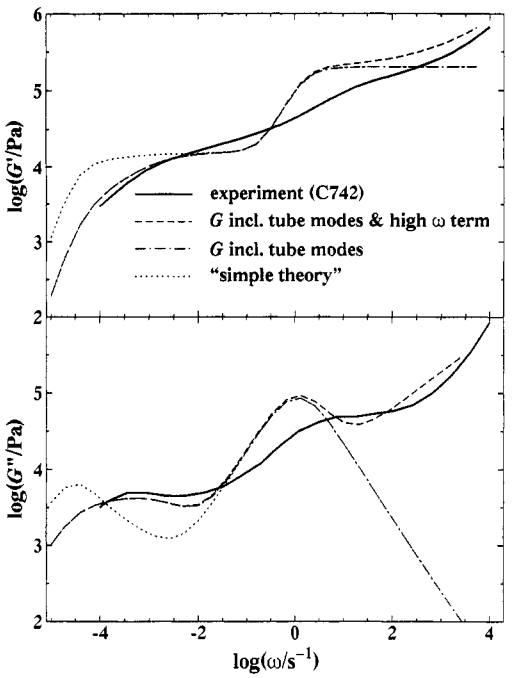

Figure 6. Frequency dependence of the storage G' (a) and loss G'' (b) moduli for the comb denoted C742 by Graessley and Roovers. The figure shows a comparison of our theory to experiments[21] for the case of mutually entangled backbones ($Q/N_e = 45$, $Q_{eff} = 15$).

reflecting these assumptions. We may note that the assumption of smaller steps between retractions is in better accord with the data. Assuming that the branch points have diffusion constants scaling as those of star polymers of the same arm molecular weight (D_{bb} is a diffusion coefficient for a lengthwise motion of the backbone), one eventually comes to

$$\tau_R \approx (Q/q - 1)^2 \frac{\tau_{br}}{\pi^2} \tag{19}$$

where the branch relaxation time is given by eq A.2.2) in Appendix 2. The storage and loss moduli (5), $G'(\omega)$ and $G''(\omega)$, have been calculated for various sets of structure parameters of a comb polymer to see how the two predicted types of behavior (i.e., for mutually entangled and for mutually diluted backbones) actually compare with experiments.

4. Discussion

In Figures 5a,b and 6a,b theoretical curves for $G(\omega)$ are plotted together with experimental data from the paper by Roovers and Graessley.[21] There are two adjustable parameters in the fit which correspond to a choice of values for the plateau modulus and monomeric friction constant and represent freedom to shift the theoretical curves in the vertical and horizontal directions. The necessary values are, however, consistent with literature values of 2.1×10^5 Pa and with the high-frequency response, respectively.

First of all, it appears that effective concentration of entanglements per backbone really is an important parameter. For example, it helps to explain the regime of linear dependence $G(\omega)$ in Figure 5 for the C642 polymer; in this case the ratio $Q/N_e \cong 14$, but $c_{eff} \cong 0.2$, so $Q_{eff} = (Q/N_e)c_{eff} \cong 3$, which means that, due to constraint release, the backbones are not densely entangled and behave themselves merely as Rouse chains. At the same time, for C742 the structure parameters are $Q/q = 29$, $n \cong 3$, $Q/N_e \cong 45$, $c_{eff} \cong 1/3$; therefore $Q_{eff} \cong 15$ and $\tau \cong (Q/q)(Q/N_e)^2 c_{eff}^2 \tau_{br} \cong 6 \times 10^3$ s, corresponding to $\omega \cong (1/6) \times 10^{-3}$ s^{-1}. This value of ω corresponds to the low-frequency maximum of the curve $G''(\omega)$ (Figure 6b). Thus the theory predicts a realistic value for the longest relaxation time τ also in the case of essentially entangled backbones.

Theoretical graphs in Figure 6 show how, by taking into consideration some additional contributions of constraint release at long times, a better agreement with experiments may be achieved. The dashed curve merely reflects the tube dilation theory described in the previous section (eqs 7 and 8). A further improvement would be to allow for lower frequency Rouse-type relaxation $\Phi_{Rt}(t)$ of the tube itself. This way of treating constraint release in reptating polymers was introduced by Graessley.[25] Instead of eq 7, this would lead us to

$$G(t) \cong [f(t)]^2 \Phi_{DE}(t) \Phi_{Rt}(t) \tag{20}$$

where

$$\Phi_{Rt}(t) = \sum_{k}^{Q/N_e} (N_e/Q) \exp(-2k^2 t/[\tau(Q/N_e)^2]) \tag{21}$$

with τ given by eq 2. Here Q/N_e is the number of entanglements per backbone, so $\tau(Q/N_e)^2$ gives the longest relaxation time for the tube. Although this is much longer than the reptation time of the backbone, this renormalized Rouse relaxation does affect the relaxation modulus because it behaves as $t^{-1/2}$ rather than the sharper $e^{-t/\tau}$ approximation to the reptation relaxation. The effects of including this process into the model are clearly visible: this calculation is represented by the dashed curve in Figure 6, which tends to show a smoother, more realistic behavior in the lower frequency range.

Meanwhile, at the higher frequency end, Rouse relaxation of the monomers would prevail:

$$\Phi_{hf}(t) \sim \sum_{j>N/N_e} \exp(-2j^2 t/\tau_R) \tag{22}$$

This is the standard unentangled stress relaxation from modes of shorter wavelength than the tube diameter. It will produce an increasing $G^*(\omega)$ rather than the plateau in G' and maximum in G'' predicted when all spatial modes of smaller scale than the tube diameter are ignored. (Here $\tau_R = \zeta N^2/(2/3)(\pi^2 kT)$ is the true Rouse time of the chain, not the long-time renormalized Rouse time for the tube of eq 20.)

The dashed curve in Figure 6 refers to more complete theory, including both longer time tube modes (eq 20) and the high-frequency term (eq 22). Despite the simplicity of the model, as one can see, it manages to catch all the main features of the experimental behavior. We observe that in all cases the experimental rheology gives broader features than the model predicts, especially at the high-frequency end of the spectrum. This is certainly due in part to the intermediate degree of entanglement of the side arms. The theory applied is true asymptotically in the limit of highly entangled arms (eq 18), and some corrections would need to be applied in the case of fewer than $5M_e$ in analogy with the entanglement crossover in linear polymers.

5. Conclusions

We suggest a more accurate form of the path length potential. It is found from a detailed description of relaxation of a branch, allowing for the tube dilation, and

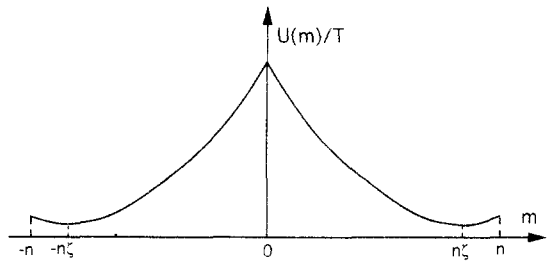

Figure 7. Effective potential $U(m)$ (see Appendix 2) as a function of the primitive path length of a branch.

then used to describe rheological properties of a comb polymer melt. A careful choice of the potential enables us to compare quantitatively the theoretical predictions (e.g., the frequency dependence of the storage and loss moduli) with experiments by other authors. We show that the effect of constraint release, as well as long-time modes of the tube itself are essential to understand some experimental data. An interesting case for further experiment would be combs with rather more highly entangled arms, for which a more highly developed spectrum of relaxation times might emerge at higher frequencies. We note further that, although the nonlinear rheology of these polymers has been treated neither experimentally nor theoretically to date, the model employed here is extendable to the case of fast-flow (ref 17). We defer this project to the near future.

Acknowledgment. We are grateful to the AFRC for financial support of our work.

Appendix 1. The Effective Potential: Logarithmic Terms

The following system of recurrent equations has been obtained for the probability distribution:[22,23]

$$P(m,N) = (z-1)P(m-1,N-1)/z + P(m+1,N-1)/z \quad \text{(A.1.1)}$$

$$P(1,N) = P(0,N-1) + P(2,N-1)/z$$

$$P(0,N) = P(1,N-1)/z$$

$$P(m,0) = \delta_{m0}$$

where z is the coordination number of the lattice.

However, the exact solution of eq A.1.1 was derived in ref 22 (as well as in refs 11 and 12) disregarding the initial and boundary conditions. But, obviously, the whole set of equations (including the initial and boundary conditions) should be considered if one wants to find a more accurate expression for $P(m,N)$. We have shown[13,14] that the careful calculation gives an additional logarithmic term in the effective potential. In fact, for $N \gg 1$ the probability distribution is

$$P(m,n) = (1/\zeta)(2/\pi)^{1/2}n^{-3/2}(m + 1/\zeta)\exp[m\zeta - n\zeta^2/2 - m^2/(2n)]$$

where $\zeta = (z-2)/z$; so, from eq 1, the corresponding potential appears to be

$$U(m)/T = (m - n\zeta)^2/(2n) - \log(m + 1/\zeta) + (3/2)\log(n) \quad \text{(A.1.2)}$$

Appendix 2. Relaxation of a Branch: Method of Kramers

Let us just assume formally that the range $m < 0$ corresponds to the situation when a backbone has moved along itself by a step of the lattice (Figure 1) and the primitive length of the branch is equal to m. Then $U(m,n) = U(-m,n)$. The function $U(m)$ is shown in Figure 7. Two minima ($m = \pm n\zeta$) can be related to two different positions of the branch in two neighboring potential wells (Figure 1). While the backbone is moving along itself and passes one step of the lattice, the branch transfers from one potential well into another one. The time of this transfer, τ_{br}, is just the reptation time. It is actually of the same order of value as the longest stress relaxation time in a star polymer melt. It can be estimated based on the method of Kramers (for a particle diffusion through a potential barrier):[17]

$$\tau_{br}(n) = (1/D)\int_{-n}^{n}\exp[U(m)/T]\,dm\int_{0}^{n}\exp[-U(m)/T]\,dm \quad \text{(A.2.1)}$$

Here D is the diffusion coefficient of the branch reptation motion; it is proportional to $(N-1)$ since the friction experienced by all the monomers along the branch actually sums up.[8]

Substituting $U(m)$ from Appendix 1, we find

$$\tau_{br} \sim N_e^{-3/2}N^{5/2}\exp(\alpha N/N_e) \quad \text{(A.2.2)}$$

where $\alpha = [(z-2)/z]^2/2$ is a parameter of the model (it is determined by the structure of the chosen network of entanglements).

It might be worth noting that the preexponential factor in the dependence $\tau_{br}(n)$ turns out to be $N^{5/2}$, which differs from the previous result $N^{3/2}$ obtained in ref 5 for the merely quadratic potential. The difference should be more essential for the combs with not too densely entangled branches.

Glossary of Symbols

$U(m)$	free energy of an entangled arm of primitive path length
a	tube diameter
l	Kuhn length
N	degree of polymerization of side branches
N_e	degree of polymerization of an entanglement strand
n	dimensionless side branch length ($=N/N_e$)
Q	degree of polymerization of the backbone
q	number of monomers between side branches
τ_{bb}	longest relaxation time of the backbone
τ_{br}	longest relaxation time of a branch
τ_{Rb}	"tube-Rouse" time for the backbone
τ_R	true Rouse time for the backbone
D	diffusion coefficient for the arm retraction
D_{bb}	effective curvilinear diffusion constant for the backbone
$f_{bb}(t)$	fraction of unrelaxed backbone at time t
$m(t)$	amount of unrelaxed arm primitive path relaxed at time t
$\Phi_{DE}(t)$	Doi–Edwards relaxation spectrum
μ_{br}	effective friction coefficient of a branch point

References and Notes

(1) Graessley, W. W. *Physical Properties of Polymers*; American Chemical Society: Washington, DC, 1984; pp 97–153.
(2) De Gennes, P.-G. *J. Phys. (Paris)* **1975**, *56*, 1199.
(3) Doi, M.; Kuzuu, N. Y. *J. Polym. Sci., Polym. Lett. Ed.* **1980**, *18*, 775.

(4) Pearson, D. S.; Helfand, E. *Faraday Symp. Chem. Soc.* **1983**, *16*, 189.
(5) Pearson, D. S.; Helfand, E. *Macromolecules* **1984**, *17*, 888.
(6) Doi, M.; Edwards, S. F. *J. Chem. Soc., Faraday Trans. 2* **1978**, *74*, 1789; **1979**, *75*, 38.
(7) Doi, M.; Edwards, S. F. *The Theory of Polymer Dynamics*; Oxford University Press: Oxford, 1986.
(8) De Gennes, P.-G. *J. Chem. Phys.* **1971**, *55*, 572.
(9) De Gennes, P.-G. *Scaling Concepts in Polymer Physics*; Cornell University Press: Ithaca, NY, 1979.
(10) Edwards, S. F. *Proc. Phys. Soc.* **1967**, *92*, 9; *J. Phys. A* **1968**, *1A*, 15.
(11) Helfand, E.; Pearson, D. S. *J. Chem. Phys.* **1983**, *79*, 2054.
(12) Rubinstein, M.; Helfand, E. *J. Chem. Phys.* **1985**, *82*, 2477.
(13) Semenov, A. N.; Yurasova, T. A. *Vysokomol. Soed.* **1987**, *29B*, 175.
(14) Yurasova, T. A.; Semenov, A. N. *Vestn. Mosk. Univ. Ser. 3: Fiz. Astron.* **1988**, *29*, 69.
(15) Mehta, A.; Needs, R. J.; Thouless, D. J. *Europhys. Lett.* **1991**, *14*, 113.
(16) Marrucci, G. J. *J. Polym. Sci., Polym. Phys. Ed.* **1985**, *23*, 159.
(17) McLeish, T. C. B. *Macromolecules* **1988**, *21*, 1062.
(18) Ball, R. C.; McLeish, T. C. B. *Macromolecules* **1989**, *22*, 1911.
(19) Kramers, H. A. *Physica A* **1940**, *7A*, 284.
(20) Roovers, J.; Toporowski, P. M. *Macromolecules* **1987**, *20*, 2300.
(21) Roovers, J., Graessley, W. W. *Macromolecules* **1981**, *14*, 766.
(22) Khokhlov, A. R.; Nechaev, S. K. *Phys. Lett.* **1985**, *112A*, 156.
(23) Nechaev, S. K.; Semenov, A. N.; Koleva, M. K. *Physica A* **1987**, *140A*, 506.
(24) Colby, R. H.; Rubinstein, M. *Macromolecules* **1990**, *23*, 2753.
(25) Graessley, W. W. *Adv. Polym. Sci.* **1982**, *47*, 67.